Slowly Inactivating Sodium Current (I_{NaP}) Underlies Single-Spike Activity in Rat Subthalamic Neurons

CORINNE BEURRIER,[1] BERNARD BIOULAC,[1] AND CONSTANCE HAMMOND[2]
[1]*Laboratoire de neurophysiologie, Centre National de la Recherche Scientifique, 33076 Bordeaux Cedex; and* [2]*Institut National de la Santé et de la Recherche Médicale U29, Institut de Neurobiologie de la Mediterranée, 13273 Marseille Cedex 09, France*

Beurrier, Corinne, Bernard Bioulac, and Constance Hammond. Slowly inactivating sodium current (I_{NaP}) underlies single-spike activity in rat subthalamic neurons. *J. Neurophysiol.* 83: 1951–1957, 2000. One-half of the subthalamic nucleus (STN) neurons switch from single-spike activity to burst-firing mode according to membrane potential. In an earlier study, the ionic mechanisms of the bursting mode were studied but the ionic currents underlying single-spike activity were not determined. The single-spike mode of activity of STN neurons recorded from acute slices in the current clamp mode is TTX-sensitive but is not abolished by antagonists of ionotropic glutamatergic and GABAergic receptors, blockers of calcium currents (2 mM cobalt or 40 μM nickel), or intracellular Ca^{2+} ions chelators. Tonic activity is characterized by a pacemaker depolarization that spontaneously brings the membrane from the peak of the afterspike hyperpolarization (AHP) to firing threshold (from -57.1 ± 0.5 mV to -42.2 ± 0.3 mV). Voltage-clamp recordings suggest that the Ni^{2+}-sensitive, T-type Ca^{2+} current does not play a significant role in single-spike activity because it is totally inactivated at potentials more depolarized than -60 mV. In contrast, the TTX-sensitive, I_{NaP} that activated at -54.4 ± 0.6 mV fulfills the conditions for underlying pacemaker depolarization because it is activated below spike threshold and is not fully inactivated in the pacemaker range. In some cases, the depolarization required to reach the threshold for I_{NaP} activation is mediated by hyperpolarization-activated cation current (I_h). This was directly confirmed by the cesium-induced shift from single-spike to burst-firing mode which was observed in some STN neurons. Therefore, a fraction of I_h which is tonically activated at rest, exerts a depolarizing influence and enables membrane potential to reach the threshold for I_{NaP} activation, thus favoring the single-spike mode. The combined action of I_{NaP} and I_h is responsible for the dual mode of discharge of STN neurons.

INTRODUCTION

The subthalamic nucleus (STN) is a basal ganglia nucleus that plays an important role in normal (Matsumara et al. 1992; Wichmann et al. 1994) and pathological (Bergman et al. 1994) motor behavior. By way of its glutamatergic projections (Smith and Parent 1988), STN imposes its rhythm to the two principal output structures of the basal ganglia, the internal pallidal segment and the substantia nigra pars reticulata (Féger et al. 1997; Parent and Hazrati 1995). In a normal in vivo situation, the great majority of rat and monkey STN neurons present a tonic activity with a frequency varying from 5 to 65 Hz and few neurons discharge in bursts (Matsumara et al. 1992; Overton and Greenfield 1995; Wichmann et al. 1994). After the onset of a conditioned movement, a period of high-frequency spikes is usually recorded (Georgopoulos et al. 1983; Matsumara et al. 1992; Miller and DeLong 1987; Wichmann et al. 1994). In a pathological situation, after a lesion of nigral dopaminergic neurons, there was an observed increase in the percentage of bursts in the discharge of STN neurons in rats and monkeys in vivo (Bergman et al. 1994; Hassani et al. 1996; Hollerman and Grace 1992) as well as in Parkinsonian patients (Benazzouz et al. 1996). We previously showed that approximately one-half of the STN neurons recorded in slices in vitro have intrinsic membrane properties that allow them to switch from a tonic to a burst-firing mode in response to membrane hyperpolarization (Beurrier et al. 1999).

This raises the question as to which conductances are altered by afferent synaptic inputs to switch the activity of STN neurons from single-spike to burst-firing mode (or the reverse). It is desirable to first identify the set of ionic currents that are of demonstrable importance in regulating the different firing modes. We previously analyzed the cascade of currents underlying burst firing mode (Beurrier et al. 1999). The aim of this study was to build up a picture of the ionic mechanisms of the tonic firing mode with the use of whole cell recordings of STN neurons in slices, in current, or voltage-clamp mode. We analyzed the ionic currents underlying the spontaneous depolarization that during the interspike interval bring the membrane potential from the peak of the afterspike hyperpolarization (AHP) to the threshold potential of Na^+ spike initiation. We now report that pacemaker depolarization mainly results from the activation of a subthreshold, slowly inactivating, TTX-sensitive Na^+ current (I_{NaP}). We also show that in approximately one-half of the neurons tested, the hyperpolarization-activated cation current (I_h) blockade hyperpolarizes the membrane sufficiently to switch STN activity to burst-firing mode, thus suggesting that the fraction of I_h opened at rest allows STN neurons to maintain a single-spike mode of activity.

METHODS

Slice preparation

Experiments were performed on STN neurons in slices obtained from 20- to 28-day-old male Wistar rats. Rats were anesthetized with ether and decapitated. The brain was removed quickly and a block of tissue containing the STN was isolated on ice in a 0–5°C oxygenated solution containing (in mM) 1.15 NaH_2PO_4, 2 KCl, 26 $NaHCO_3$, 7 $MgCl_2$, 0.5 $CaCl_2$, 11 glucose, and 250 saccharose, equilibrated with 95% O_2-5% CO_2 (pH 7.4). This cold solution, with a low NaCl and $CaCl_2$ content, improved tissue viability. In the same medium, 300- to

The costs of publication of this article were defrayed in part by the payment of page charges. The article must therefore be hereby marked "*advertisement*" in accordance with 18 U.S.C. Section 1734 solely to indicate this fact.

400-μm thick coronal slices were prepared using a vibratome (Campden Instruments, Loughborough, UK) and were incubated at room temperature in a Krebs solution containing (in mM) 124 NaCl, 3.6 KCl, 1.25 HEPES, 26 $NaHCO_3$, 1.3 $MgCl_2$, 2.4 $CaCl_2$, and 10 glucose, equilibrated with 95% O_2-5% CO_2 (pH 7.4). After a 2-h recovery period, STN slices were transferred one at a time to an interface-type recording chamber, maintained at 30 ± 2 °C, and continuously superfused (1–1.5 $ml \cdot min^{-1}$) with the oxygenated Krebs solution.

Electrophysiological recordings

Slices were viewed using a dissecting microscope and the recording electrode was precisely positioned in the STN. Electrophysiological recordings of STN neurons were performed in current or in voltage-clamp mode using the blind patch-clamp technique in the whole cell configuration. Patch electrodes were pulled from filamented borosilicate thin-wall glass capillaries (GC150F-15, Clarck Electromedical Instruments, Pangbourne, UK) with a vertical puller (PP-830, Narishige, Japan) and had a resistance of 10 to 12 MΩ when filled with *solution 1* (see *Intracellular solutions*).

Intracellular solutions

For current-clamp recordings a K-gluconate-based solution (*solution 1*) was used. It contained (in mM) 120 K-gluconate, 10 KCl, 10 NaCl, 10 EGTA, 10 HEPES, 1 $CaCl_2$, 2 MgATP, and 0.5 NaGTP (pH 7.25). To study low-threshold voltage-activated T-type Ca^{2+} current (I_{CaT}), the 120 mM K-gluconate in *solution 1* was substituted for an equimolar concentration of CsCl and KCl was omitted as was ATP and GTP to reduce the L-type Ca^{2+} current which is known to be sensitive to run-down (*solution 2*). In some experiments the Ca^{2+} chelator 1,2-bis(2-aminophenoxy)-ethane-*N*,*N*,*N*′,*N*′-tetraacetic acid, tetrapotassium salt (BAPTA, 10 mM) was added to *solution 1* which contained 80 mM K-gluconate instead of 120 mM to obtain an osmolarity ~270 $mOsm \cdot l^{-1}$. In this solution, the Ca^{2+} ion concentration was decreased from 1 to 0.1 mM (*solution 3*). To record Na^+ currents, the 120 mM K-gluconate in solution 1 was substituted for an equimolar concentration of CsCl and KCl was omitted (*solution 4*).

Extracellular solutions

For voltage-clamp experiments, the Krebs solution contained 1 μM TTX, 3 μM nifedipine, and 1 mM Cs^+ for the I_{CaT} study (*solution A*). For the I_{NaP} study, 2 mM Co^{2+} and 1 mM Cs^+ were added and the Ca^{2+} ions concentration was decreased from 2.4 to 0.5 mM (*solution B*). For the I_h study, 1 μM TTX was added (*solution C*).

Drugs

All drugs were purchased from Sigma (St. Louis, MO), except 6-cyano-7-nitroquinoxaline-2,3-dione (CNQX), D-(−)-2-amino-5-phosphopentanoic acid (D-APV), and bicuculline which were purchased from Tocris (Bristol, UK). BAPTA was diluted in the pipette solution. All other drugs were diluted in the oxygenated Krebs and applied through this superfusion medium. Nifedipine and CNQX were dissolved in dimethylsulfoxide (final concentration, 0.03–0.3%).

Data analysis

Membrane potential was recorded using an Axoclamp 2A or Axopatch 1D amplifier (Axon Instuments, Foster City, CA), displayed simultaneously on a storage oscilloscope and a four-channel chart recorder (Gould Instruments, Longjumeau, France), digitized (DR-890, NeuroData Instruments, NY), and stored on a videotape for subsequent offline analysis. In voltage-clamp experiments, membrane currents were amplified by an Axopatch 1D or an Axoclamp 2A, fed into an A/D converter (Digidata 1200, Axon Instuments), and stored and analyzed on a PC using pCLAMP software (version 6.0.1, Axon Instruments). Because different recording solutions were used throughout the study, corrections for the liquid junction potential were performed. The correction was −6 mV for the K-gluconate-based pipette solution as estimated with a 3 M KCl ground electrode (Neher 1992).

RESULTS

Data presented here are based on patch-clamp recordings of 155 STN neurons. Neuronal activity was recorded in current-clamp mode ($n = 57$) and subthreshold currents were recorded in voltage-clamp mode (whole cell configuration, $n = 106$).

Characteristics of single-spike activity and pacemaker depolarization

All STN neurons displayed a single-spike mode of Na^+ action potentials (Fig. 1*A*) that was totally abolished in the

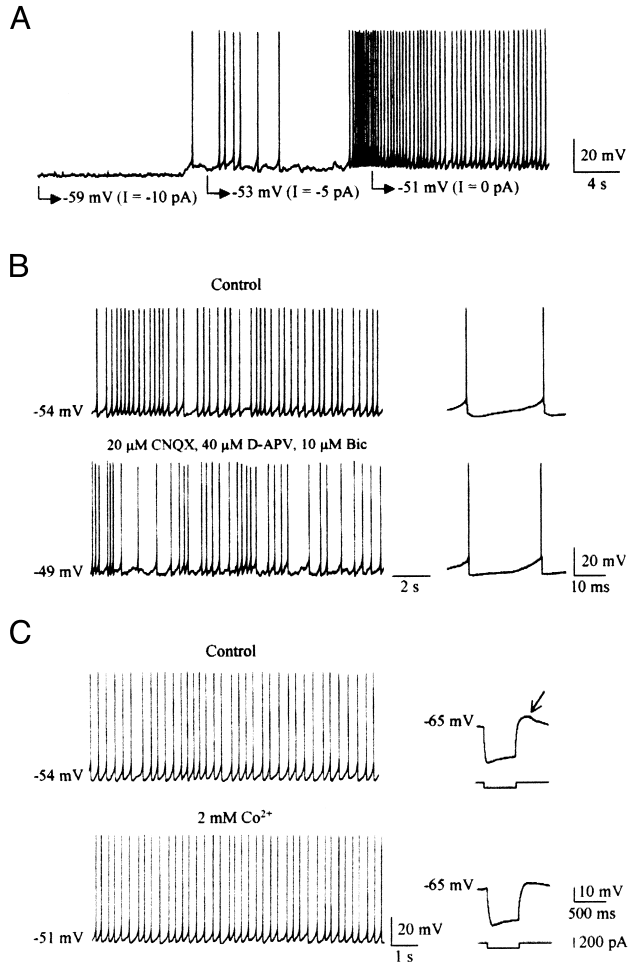

FIG. 1. Single-spike activity of subthalamic nucleus (STN) neurons. *A*: dependence on membrane potential. Tonic activity present at resting membrane potential ($I = 0$ pA), decreased in frequency at a more hyperpolarized potential ($I = -5$ pA), and stopped ($I = -10$ pA). *B* and *C*: dependence on synaptic activity. A bath application of blockers of AMPA/kainate (CNQX), NMDA (D-APV), and $GABA_A$ (bicuculline) receptors and of voltage-activated Ca^{2+} currents (Co^{2+}) did not block single-spike activity. *Inset* in *B* shows 2 traces of pacemaker depolarization in control (*top*) and treated (*bottom*) conditions. *Insets* in *C* show the low-threshold Ca^{2+} spike at the break of a hyperpolarizing pulse in control (arrow, *top*) and during Co^{2+} application (*bottom*). External Krebs, intrapipette *solution 1*.

presence of 1 μM TTX. Action potentials had a mean threshold of -42.2 ± 0.3 mV (range: -45 to -40 mV, $n = 24$) and were followed by an AHP that peaked at -57.1 ± 0.5 mV (range: -54 to -62 mV, $n = 25$). Between consecutive spikes, the membrane spontaneously depolarized by ~15 mV from the peak of the AHP to the threshold potential of the following spike (Fig. 1*B*, control *inset*). By analogy with the pacemaker activity of cardiac cells, we called this phase "pacemaker depolarization" (DiFrancesco 1993). The mean frequency was 7.6 ± 0.8 Hz (range: 5.0–17.1 Hz, $n = 16$) in the absence of current injection. When cells were hyperpolarized by negative current injection, approximately one-half of the recorded STN neurons shifted to burst-firing mode (Beurrier et al. 1999) with an AHP peaking at -61.8 ± 0.8 mV (range: -58 to -72 mV, $n = 20$) whereas the remaining one-half displayed single-spike mode but at lower frequencies (Fig. 1*A*). At more hyperpolarized potentials both types of STN neurons were silent (Fig. 1*A*).

Single-spike mode was not blocked by a concomitant application of CNQX, D-APV, and bicuculline, the respective antagonists of AMPA/kainate, NMDA, and $GABA_A$ ionotropic receptors (Fig. 1*B*, $n = 6$), neither was it suppressed by cobalt (Fig. 1*C*, Co^{2+} 2 mM, $n = 32$). These findings showed that the TTX-sensitive, voltage-dependent single-spike activity is independent of afferent synaptic activity (and particularly activation of glutamatergic and GABAergic ionotropic receptors). This raised the possibility that single-spike activity results from intrinsic voltage-dependent properties of the membrane (i.e., from currents underlying the pacemaker depolarization of the interspike interval that spontaneously brings the membrane potential from the peak of the AHP to the threshold potential for Na^+-spike initiation). During this phase, the net current is inward because a decreasing outward current cannot by itself depolarize the membrane to Na^+-spike threshold (Irisawa et al. 1993). Moreover, inward currents are more efficient in depolarizing the membrane whereas outward currents are decreasing and membrane resistance is thus increased. More precisely, increase of resistance depends on the density and deactivation characteristics (kinetics and voltage dependence) of outward currents open at the peak of the AHP. The subthreshold inward currents we analyzed were I_{CaT}, Ca^{2+}-activated inward (cationic) currents (I_{CAN}), I_{NaP}, and I_h. To identify which of these currents was involved, we studied the effects of their pharmacological blockade in current-clamp mode and analyzed their voltage dependence in voltage-clamp mode. Does the membrane reach a level of depolarization sufficient for this current to be activated during the interspike interval? Does this current inactivate during repetitive firing?

I_{CaT}

Nickel chloride at a concentration (Ni^{2+}, 40 μM) that preferentially blocks T-type Ca^{2+} currents (Huguenard 1996) (Fig. 2*B*) did not affect single-spike activity (Fig. 2*A*, $n = 28$) but strongly reduced the rebound potential called low-threshold Ca^{2+} spike (Nakanishi et al. 1987) seen at the break of a hyperpolarizing current pulse (Fig. 2*A*, *insets*). This is consistent with above observations that single-spike activity was still present under 2 mM Co^{2+} (Fig. 1*C*). Voltage-clamp experiments were performed in the presence of L-type Ca^{2+} current blockers (see METHODS *solutions A* and *2*). Currents were

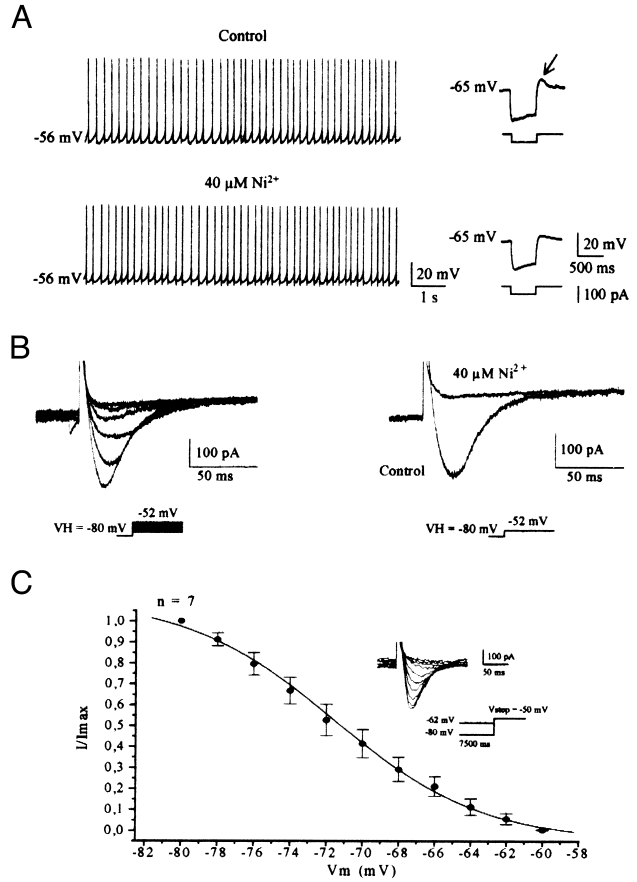

FIG. 2. Single-spike activity is not mediated by low-threshold T-type Ca^{2+} current (I_{CaT}). *A*: a bath application of Ni^{2+} (40 μM) did not affect tonic activity recorded in current clamp mode though it strongly reduced the amplitude of rebound potential evoked at break of a 500-ms hyperpolarizing pulse to -88 mV (*insets*). *B*: inward Ca^{2+} currents recorded in response to 200-ms depolarizing steps from -62 to -52 mV (2 mV increment, $V_H = -80$ mV, *left*) were strongly depressed by Ni^{2+} (*right*, step to -52 mV). Inactivation was fitted with a double exponential ($\tau_1 = 13.0$ and $\tau_2 = 165.7$ ms). *C*: steady state inactivation curve obtained from current traces shown in *inset*: 7,500-ms conditioning prepulses from -80 to -62 mV (2 mV increment) were followed by a fixed 200-ms step to -50 mV. Currents were normalized (I/I_{max}) to maximal current (I_{max}) recorded at -80 mV. Data were fitted with a smooth curve derived from the Boltzmann equation ($V_{1/2}$ of inactivation = -71.6 mV and slope factor $k = 4.1$, $n = 7$). *A*: external Krebs and intrapipette *solution 1*. *B* and *C*: external solution A and intrapipette solution 2.

evoked by step depolarizations to varying test potentials from a holding potential of -80 mV. A low voltage-activated inward current that had the characteristics of I_{CaT} was recorded; it activated at -59.3 ± 0.7 mV (range: -62 to -55 mV, $n = 10$), presented a rather slow kinetic of inactivation (Fig. 2*B*, *left*), and was totally abolished in the presence of 40 μM Ni^{2+} (Fig. 2*B*, *right*). After a 7.5-s conditioning step at -59.9 ± 2.3 mV (range: -66 to -45 mV, $n = 8$), it was fully inactivated (Fig. 2*C*). Because I_{CaT} is totally inactivated at potentials crossed by the membrane during repetitive discharge, it is unlikely that it participates significantly to the slow pacemaker depolarization.

Calcium-activated inward currents

BAPTA (10 mM), a Ca^{2+} chelator, was introduced into the pipette solution (*solution 3*) to test the participation of Ca^{2+}-

activated currents such as I_{CAN}, a current that is inward in the potential range of the pacemaker depolarization (Crépel et al. 1994). In agreement with our previous results (Beurrier et al. 1999), BAPTA did not affect single-spike mode (Fig. 3, $n = 5$) although it effectively blocked Ca^{2+}-activated inward current as shown by the strong reduction of the plateau potential duration evoked by a depolarizing current pulse (Fig. 3, *insets*). This suggested that Ca^{2+}-activated currents are not absolutely necessary to sustain single-spike activity. However, they may be activated by a single spike and contribute to the pacemaker depolarization.

I_{NaP}

I_{NaP} is a TTX-sensitive Na^+ current that activates below spike threshold and slowly inactivates (Crill 1996). The role of I_{NaP} on the pattern of discharge in current-clamp recordings is difficult to study because the pharmacological substances that block it (e.g., TTX or QX 314, a derivative of lidocaine) are also blockers of the Na^+ spike. The role of I_{NaP} in the pacemaker depolarization was deduced from the analysis of its voltage dependence. Two protocols were used, either a depolarizing ramp (Fig. 4*A*, speed 5 mV · s^{-1}) or long depolarizing steps (1,500 ms) of increasing amplitude (Fig. 4*B*). K^+ currents were reduced by replacing K^+ ions by Cs^+ in the pipette solution (*solution 4*) and by adding 1 mM Cs^+ in the bath medium. Ca^{2+} currents were suppressed by adding 2 mM Co^{2+} in the bath medium and by decreasing the external concentration of Ca^{2+} ions (*solution B*). In response to the voltage ramp, an inward current that had the characteristics of a persistent Na^+ current (I_{NaP}) was recorded; it activated at -54.4 ± 0.6 mV (range: -57.2 to -50.3 mV), peaked at -32.9 ± 0.8 mV (range: -37.4 to -26.8 mV), had a maximal amplitude of -211.1 ± 8.5 pA (range: -266.1 to -164.2 pA), and was totally abolished in the presence of 1 μM TTX (Fig. 4*A*, $n = 13$). Because I_{NaP} peaked fast during the ramp protocol, probably because it came out of voltage control and because I_{NaP} can partially

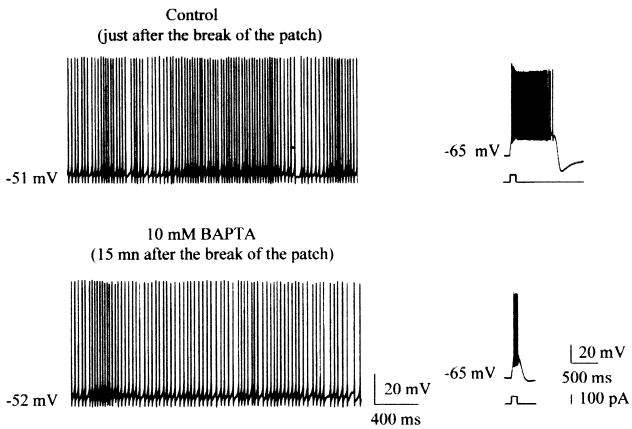

FIG. 3. Single-spike activity does not depend on Ca^{2+}-activated currents. BAPTA (10 mM), the Ca^{2+} chelator, was present in the pipette solution. Single-spike activity was recorded in current clamp mode (whole cell configuration) just after breaking through the patch of membrane (control) when BAPTA had not yet diffused into the cell as shown by the presence of plateau potential in response to a depolarizing current pulse (*inset*). Fifteen minutes later (*bottom*), plateau potential was strongly reduced (*inset*) but tonic activity was still present. External Krebs and intrapipette *solution 3*.

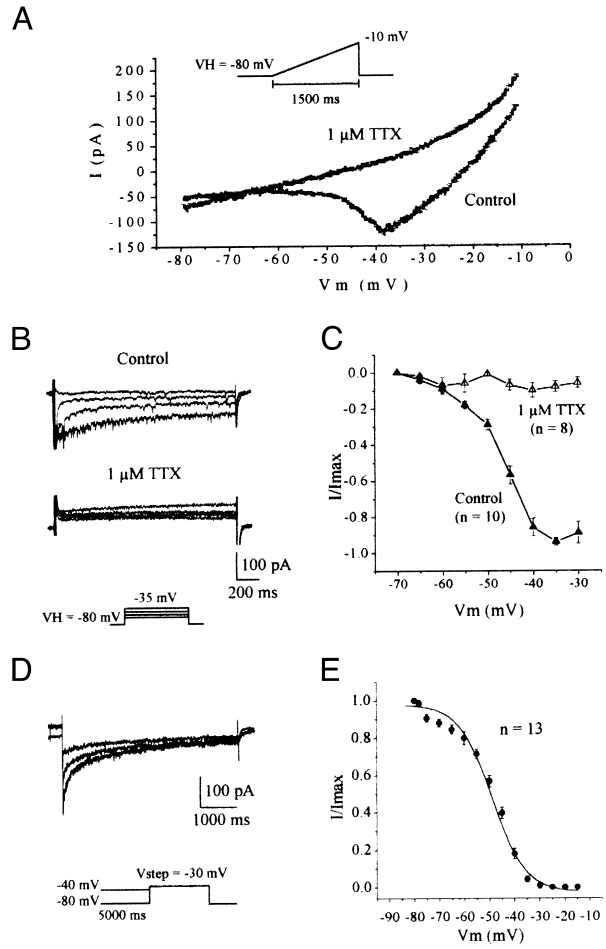

FIG. 4. Persistent TTX-sensitive Na^+ current (I_{NaP}). *A*: current response to a voltage ramp applied at 5 mV · s^{-1} in absence (control) and presence (TTX) of 1 μM TTX. Outward current is present in both situations as a result of the absence of blockers of delayed rectifier K^+ current in extracellular medium. *B*: currents evoked by 1,500-ms step commands from -70 to -30 mV (from *bottom* to *top*, steps to -60, -55, -50, and -35 mV) in control conditions (control) and in presence of TTX. *C*: *I-V* relationship obtained with a protocol similar to that in *B*. Leak and outward currents were subtracted. Current amplitudes were normalized (I/I_{max}) to maximal current (I_{max}) recorded. *D*: current responses to a 5-s step to -30 mV preceded by a 5-s conditioning pulse from -80 to -40 mV (from *bottom* to *top* conditioning pulses at -75, -50, and -40 mV). *E*: steady-state inactivation curve of I_{NaP} obtained with a protocol similar to that in *D*. Current amplitudes were measured 300 ms after onset of depolarization and were normalized (I/I_{max}) to maximal current (I_{max}) recorded (leak was subtracted). Data were fitted with a smooth curve derived from the Boltzmann equation ($V_{1/2}$ of inactivation = -48.8 mV and slope factor $k = 6.5$ mV, $n = 7$). External solution B and intrapipette *solution 4*. Fast Na^+ current was truncated in *B* and *D*.

inactivate during the time course of the ramp command, the voltage step protocol was also tested. From a holding potential of -80 mV, a slowly inactivating Na^+ current was observed (Fig. 4*B*). It activated from -56.9 ± 1.3 mV (range: -60 to -50 mV, $n = 10$) and was totally abolished in the presence of 1 μM TTX (Fig. 4, *B* and *C*). I_{NaP} inactivated slowly (~20%) during a 5-s voltage step at -42 mV ($V_H = -60$ mV, $n = 5$, data not shown). Voltage-dependent steady-state inactivation was studied with the protocol shown in Fig. 4*D*. After 5 s at approximately -50 mV ($n = 13$), I_{NaP} was one-half inactivated and after 5 s at -30 mV was fully inactivated (Fig. 4, *D* and *E*). To approach the situation during regular spiking, another protocol

was tested. A situation where the membrane was rather depolarized was chosen; from a holding potential of −50 mV (to mimick the AHP), a 1-ms step to +20 mV was applied (to mimic a spike) and was followed by a 5-s step to −35 mV (to evoke I_{NaP} and measure channel availability). The two steps were separated by an interval of variable duration (15–60 ms) at −50 mV (to mimic the interspike interval) (Fig. 5, *left*). It was noteworthy that I_{NaP} was not inactivated by the first depolarizing pulse but also that it had a larger amplitude at shorter intervals. Further increases in interval duration gave a stable 30% reduction of I_{NaP} (Fig. 5, *right*). In conclusion, I_{NaP} activates in a potential range crossed by the membrane during the interspike interval and is not totally inactivated after a spike.

I_h

The cesium-sensitive cation current I_h is turned on by membrane hyperpolarization and is inward (depolarizing) at potentials more hyperpolarized than its reversal potential (approximately −30 mV) (Pape 1996). In ~50% of the neurons tested (n = 5 of 11), adding cesium chloride (Cs^+, 1–3 mM) to external Krebs solution hyperpolarized the membrane by approximately −12 mV and switched their activity from tonic-firing to burst-firing mode (Fig. 6*A*). When positive current was injected, tonic activity reappeared though I_h was still blocked (Fig. 6*A*, *bottom right and inset*). In the remaining one-half of the cells, Cs^+ did not affect membrane potential or tonic activity (n = 6).

Characteristics of I_h were studied in current-clamp and voltage-clamp modes (*solutions C* and *1*). In response to long hyperpolarizing currents pulses (500 ms), a time-dependent, Cs^+-sensitive anomalous rectification, seen as a slowly developing depolarizing sag, was observed (Fig. 6*A*, *insets*). This sag corresponded in voltage-clamp recordings to a slowly developing inward current that activated at −56.5 ± 0.8 mV (range: −60 to −55 mV, n = 10) in response to hyperpolarizing steps from a holding potential of −45 mV and increased in amplitude with membrane hyperpolarization (Fig. 6, *B* and *C*). This current was strongly depressed in the presence of 1 to 3 mM external Cs^+ (Fig. 6, *B* and *C*). From the above results we conclude that I_h is not essential for a tonic mode of discharge. However, in some cells it contributes toward maintaining membrane potential at a more depolarized value where tonic mode is present.

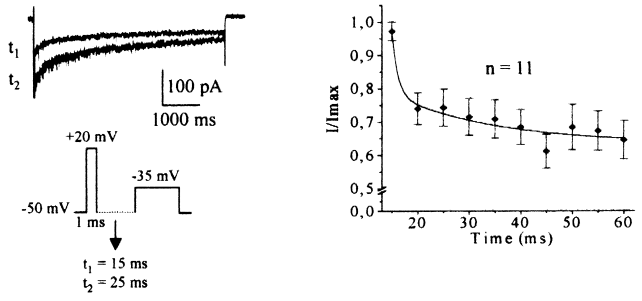

FIG. 5. I_{NaP} inactivation after a spike. Intensity of I_{NaP} in response to a 5-s depolarizing step to −35 mV was studied at different times (15–60 ms) after a short (1 ms) depolarizing step to +20 mV (V_H = −50 mV). I_{NaP} current traces (*left*) and I_{NaP} amplitude normalized (I/I_{max}) to maximal current (I_{max}) recorded after interval t = 15 ms vs. interval duration (*right*). Data were fitted with a monoexponential curve. External solution B and intrapipette *solution 4*.

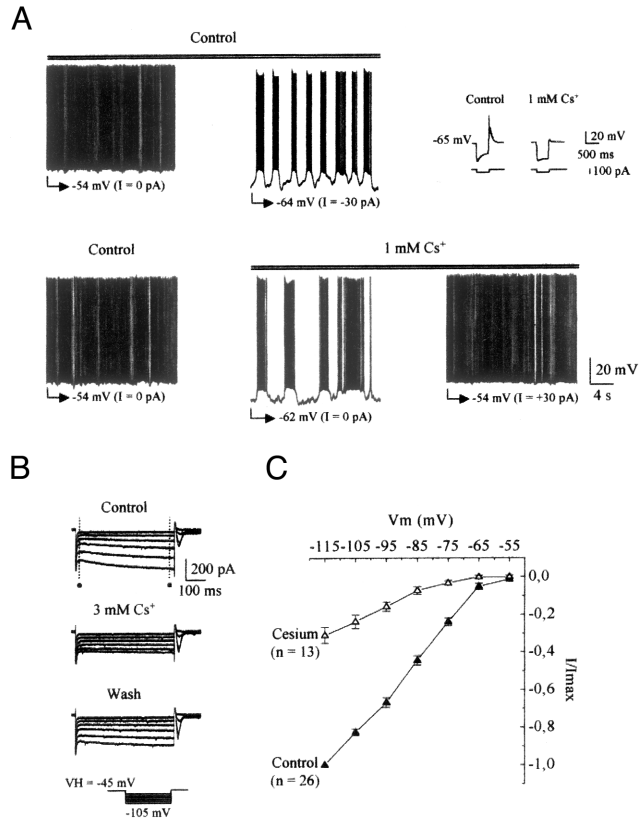

FIG. 6. Role of Cs^+-sensitive I_h current on membrane potential and firing mode. *A*: in control conditions, a STN neuron diplayed single-spike activity at resting membrane potential (I = 0 pA) and burst firing mode at more hyperpolarized potentials (*top*, control). In the same neuron, bath application of Cs^+ at resting potential hyperpolarized the membrane by 8 mV and shifted STN activity to burst firing mode (in the absence of any current injection). Continuous injection of positive current shifted back membrane potential to control value and to single-spike activity though Cs^+ was still present (*bottom*). Concomitantly, in the presence of Cs^+ the depolarizing sag recorded in response to a negative current pulse was strongly decreased as well as the depolarizing rebound seen at the break of the hyperpolarizing pulse; spike was truncated (*inset*, *left*). *B*: from a holding potential (V_H) of −45 mV, a family of currents was evoked in response to 1,500-ms hyperpolarizing steps from −55 to −105 mV (10 mV increment, *left column*) in control conditions (*top*), after bath application of Cs^+ (*middle*), and after recovery from Cs^+ (*bottom*). *C*: *I-V* relationship in absence (control) and presence of cesium (1–3 mM). Values of I are obtained by subtracting value of current at the beginning of trace (●) from that at end of trace (■). Currents were normalized (I/I_{max}) to the maximal current (I_{max}) recorded at −115 mV. *A*: external Krebs and intrapipette solution 1. *B*: external solution C and intrapipette solution 1.

DISCUSSION

These results show that single-spike activity of STN neurons is independent of afferent synaptic activity and of Ca^{2+} or Ca^{2+}-activated currents. It mainly results from the persistent Na^+ current, I_{NaP}. Moreover, in some neurons a sustained fraction of I_h exerts a depolarizing influence, enables the membrane potential to reach the threshold for I_{NaP} activation and thus favors the single-spike mode of discharge. The role of I_{NaP} in STN neurons has been deduced from its voltage-dependent characteristics whereas that of I_h was also deduced from the effect of its blockade by external Cs^+.

I_{NaP} underlies the pacemaker depolarization in the single-spike mode

We propose that the pacemaker depolarization that precedes each action potential is mainly mediated by the slowly inactivating Na^+ current, I_{NaP}. Single-spike mode is voltage-dependent and both action potentials and pacemaker depolarizations were abolished by TTX, a specific blocker of voltage-sensitive Na^+ currents whereas they were insensitive to blockers of Ca^{2+} currents. These observations can be linked to voltage-clamp experiments where a TTX-sensitive inward current recorded in all STN neurons tested, activated at voltages clearly below spike threshold and normally traversed by spontaneously firing cells. This current represented I_{NaP} because there was no residual current in the presence of TTX and a contribution of Ca^{2+} currents is most unlikely in the presence of cobalt and very low concentrations of Ca^{2+} in the extracellular medium. Interestingly, nonbursting STN neurons were silent at voltages more hyperpolarized than the I_{NaP} threshold of activation. However, insights into the functional relevance of I_{NaP} for single-spike activity need also to consider its inactivation properties. I_{NaP} could still be evoked a few milliseconds after a short depolarization that mimicked a spike.

Comparison with other preparations where I_{NaP} plays also a role in spontaneous tonic firing showed that the voltage range of I_{NaP} activation threshold in our experiments is ~5–10 mV more positive than that found in other central neurons such as neocortical layer V pyramidal neurons (Stafstrom et al. 1985), medial entorhinal neurons (Alonso and Llinas 1989), suprachiasmatic neurons (Pennartz et al. 1997), Purkinje cells (Llinas and Sugimori 1980), and hippocampal neurons (French et al. 1990; MacVicar 1985).

I_{CaT} recorded in this study does not play a significant role in single-spike mode because it is inactivated at potentials where STN neurons fire tonically. Kinetic of inactivation of I_{CaT} recorded in this study is close to that described for a T current mediated by the recently cloned α1l subunit (Lee et al. 1999), which transcript is highly expresssed in the STN (Talley et al. 1999).

Role of a sustained I_h component

We suggest that a sustained component of the Cs^+-sensitive I_h, open at resting membrane potential, contributes toward maintaining single-spike firing in some STN neurons. This is important because the value of membrane potential critically determines the pattern of firing of STN neurons (Beurrier et al. 1999). Cs^+ produced a hyperpolarization that was large enough to move the cell into the burst mode of action potential generation. This was only observed for cells that displayed a plateau potential in control conditions. We have certainly underestimated I_h amplitude and the effects of its blockade with the use of gluconate ions in the pipette solution. Gluconate ions give more physiological recordings but are known to inhibit I_h (Velumian et al. 1997). Moreover, it could also be argued that external Cs^+ also affects delayed and inward rectifier K^+ currents. However, because these currents are outward, their blockade will result in membrane depolarization instead of hyperpolarization. We can hypothesize that a sustained component of I_h as a result of its depolarizing influence moves the membrane potential from a range of Ca^{2+}-mediated burst activity into a region where it activates I_{NaP} and allows a single-spike mode of discharge. Such a contribution of I_h to resting parameters has already been described in thalamic relay neurons, cells that also display two intrinsic modes of discharge depending on membrane potential (McCormick and Pape 1990; Pape 1996). For the fraction of I_h that is activated on hyperpolarization and deactivated with depolarization, most of its depolarizing effect would be efficient at hyperpolarized potentials when STN neurons are discharging in the bursting mode. One remarkable feature of I_h channels is the presence of a cyclic nucleotide binding region that allows I_h to be modulated by second messengers. Cyclic AMP or cyclic GMP increase I_h channels activities by shifting their activation curve to more depolarized values (Ludwig et al. 1999; Santoro et al. 1998). The modulation of the voltage dependence of I_h through the production of cAMP would thus have important consequences on the firing pattern of STN neurons.

We propose that STN activity shifts from burst-firing mode to single-spike activity in response to a depolarization which induces inactivation of the calcium conductances such as I_{CaT} (which cannot generate any more slow membrane oscillations) and activation of the subthreshold depolarizing currents I_h and I_{NaP}. Conversely, tonic-firing mode would cease once the membrane is more hyperpolarized than the I_{NaP} threshold of activation. Therefore the increase in the percentage of bursts recorded in the STN after the experimental lesion of nigral dopaminergic neurons (Bergman et al. 1994; Hassani et al. 1996; Hollerman and Grace 1992) or in the absence of dopaminergic neurons (Plenz and Kitai 1999) would result from a synaptically driven hyperpolarizing shift of the background resting potential of STN neurons.

Present address of C. Beurrier: Stanford University, School of Medicine, Dept. of Psychiatry and Behavioral Sciences, 1201 Welch Rd., Palo Alto, CA 94304-5485.

Address for reprint requests: C. Hammond, INSERM U29, INMED, Route de Luminy, BP13, 13273 Marseille Cedex 09, France.

Received 20 September 1999; accepted in final form 29 November 1999.

NOTE ADDED IN PROOF

Since this paper was submitted for publication, a report by Bevan et al. was published (*J. Neurosci.* 19: 7617–7628, 1999) showing also that I_{NaP} plays a role in the tonic mode of discharge of STN neurons. However, the contribution of I_h has not been studied by the authors.

REFERENCES

ALONSO, A. AND LLINAS, R. R. Subthreshold Na^+-dependent theta like rhythmicity in stellate cells of entorhinal cortex layer II. *Nature* 342: 175–177, 1989.

BENAZZOUZ, A., BORAUD, T., FÉGER, J., BURBAUD, P., BIOULAC, B., AND GROSS, C. Alleviation of experimental hemiparkinsonism by high-frequency stimulation of the subthalamic nucleus in primates: a comparison with L-Dopa treatment. *Mov. Disord.* 11: 627–632, 1996.

BERGMAN, H., WICHMANN, T., KARMON, B., AND DELONG, M. R. The primate subthalamic nucleus. II. Neuronal activity in the MPTP model of parkinsonism. *J. Neurophysiol.* 72: 507–520, 1994.

BEURRIER, C., CONGAR, P., BIOULAC, B., AND HAMMOND, C. Subthalamic nucleus neurons switch from single-spike activity to burst-firing mode. *J. Neurosci.* 19: 599–609, 1999.

CRÉPEL, V., ANIKSZTEJN, L., BEN ARI, Y., AND HAMMOND, C. Glutamate metabotropic receptors increase a Ca^{2+}-activated non specific cationic current in CA1 hippocampal neurons. *J. Neurophysiol.* 72: 1561–1569, 1994.

CRILL, W. E. Persistent sodium current in mammalian central neurons. *Annu. Rev. Physiol.* 58: 349–362, 1996.

DIFRANCESCO, D. Pacemaker mechanisms in cardiac tissue. *Annu. Rev. Physiol.* 55: 455–472, 1993.

FÉGER, J., HASSANI, O. K., AND MOUROUX, M. The subthalamic nucleus and its connections. New electrophysiological and pharmacological data. *Adv. Neurol.* 74: 31–43, 1997.

FRENCH, C. R., SAH, P., BUCKETT, K. J., AND GAGE, P. W. A voltage-dependent persistent sodium current in mammalian hippocampal neurons. *J. Gen. Physiol.* 95: 1139–1157, 1990.

GEORGOPOULOS, A. P., DELONG, M. R., AND CRUTCHER, M. D. Relations between parameters of step-tracking movements and single cell discharge in the globus pallidus and subthalamic nucleus of the behaving monkey. *J. Neurosci.* 3: 1586–1598, 1983.

HASSANI, O. K., MOUROUX, M., AND FÉGER, J. Increased subthalamic neuronal activity after nigral dopaminergic lesion independent of disinhibition via the globus pallidus. *Neuroscience* 72: 105–115, 1996.

HOLLERMAN, J. R. AND GRACE, A. A. Subthalamic nucleus cell firing in the 6-OHDA-treated rat: basal activity and response to haloperidol. *Brain Res.* 590: 291–299, 1992.

HUGUENARD, J. R. Low-threshold calcium currents in central nervous system neurons. *Annu. Rev. Physiol.* 58: 329–348, 1996.

IRISAWA, H., BROWN, H. F., AND GILES, W. Cardiac pacemaking in the sinoatrial node. *Physiol. Rev.* 73: 197–227, 1993.

LEE, J. H., DAUD, A. N., CRIBBS, L. L., LACERDA, A. E., PEREVERZEV, A., KLÖCKNER, U., SCHNEIDER, T., AND PEREZ-REYES, E. Cloning and expression of a novel member of the low voltage-activated T-type calcium channel family. *J. Neurosci.* 19: 1912–1921, 1999.

LLINAS, R. AND SUGIMORI, M. Electrophysiological properties of in vitro Purkinje cell somata in mammalian cerebellar slices. *J. Physiol. (Lond.)* 305: 171–195, 1980.

LUDWIG, A., ZONG, X., STIEBER, J., HULLIN, R., HOFMANN, F., AND BIEL, M. Two pacemaker channels with profoundly different activation kinetics. *EMBO J.* 18: 2323–2329, 1999.

MACVICAR, B. A. Depolarizing potentials are Na^+-dependent in CA1 pyramidal neurons. *Brain Res.* 333: 378–381, 1985.

MATSUMARA, M., KOJIMA, J., GARDINER, T. W., AND HIKOSADA, O. Visual and oculomotor functions of monkey subthalamic nucleus. *J. Neurophysiol.* 67: 1615–1632, 1992.

MCCORMICK, D. A. AND PAPE, H. C. Properties of hyperpolarization-activated cation current and its role in rhythmic oscillation in thalamic relay neurones. *J. Physiol. (Lond.)* 431: 291–318, 1990.

MILLER, W. C. AND DELONG, M. R. Altered tonic activity of neurons in the globus pallidus and subthalamic nucleus in the primate MPTP model parkinsonian. In: *The Basal Ganglia II. Structure and function: current concept*, edited by M. B. Carpenter and A. Jayaraman. New York: Plenum, 1987.

NAKANISHI, H., KITA, H., AND KITAI, S. T. Electrical membrane properties of rat subthalamic neurons in an in vitro slice preparation. *Brain Res.* 437: 35–44, 1987.

NEHER, E. Correction for liquid junction potentials in patch clamp experiments. *Meth. Enzymol.* 207: 123–131, 1992.

OVERTON, P. G. AND GREENFIELD, S. A. Determinants of neuronal firing pattern in the guinea-pig subthalamic nucleus: an in vivo and in vitro comparison. *J. Neural Transm.* 10: 41–54, 1995.

PAPE, H. Queer current and pacemaker: the hyperpolarization-activated cation current in neurons. *Annu. Rev. Physiol.* 58: 299–327, 1996.

PARENT, A. AND HAZRATI, L. N. Functional anatomy of the basal ganglia. II. The place of subthalamic nucleus and external pallidum in basal ganglia circuitry. *Brain Res. Rev.* 20: 128–154, 1995.

PENNARTZ, C.M.A., BIERLAAGH, M. A., AND GEURTSEN, A.M.S. Cellular mechanisms underlying spontaneous firing in rat suprachiasmatic nucleus: involvement of a slowly inactivating component of sodium current. *J. Neurophysiol.* 78: 1811–1825, 1997.

PLENZ, D. AND KITAI, S. T. A basal ganglia pacemaker formed by the subthalamic nucleus and external globus pallidus. *Nature* 400: 677–682, 1999.

SANTORO, B., LIU, D. T., YAO, H., BARTSCH, D., KANDEL, E. R., SIEGELBAUM, S. A., AND TIBBS, G. R. Identification of a gene encoding a hyperpolarization-activated pacemaker channel of brain. *Cell* 93: 717–729, 1998.

SMITH, Y. AND PARENT, A. Neurons of the subthalamic nucleus in primates display glutamate but not GABA immunoreactivity. *Brain Res.* 453: 353–356, 1988.

STAFSTROM, C. E., SCHWINDT, P. C., CHUBB, M. C., AND CRILL, W. E. Properties of persistent sodium conductance and calcium conductance of layer V neurons from cat sensorimotor cortex. *J. Neurophysiol.* 53: 153–170, 1985.

TALLEY, E. M., CRIBBS, L. L., LEE, J. H., DAUD, A., PEREZ-REYES, E., AND BAYLISS, D. A. Differential distribution of three members of a gene family encoding low voltage-activated (T-type) calcium channels. *J. Neurosci.* 19: 1895–1911, 1999.

VELUMIAN, A. A., ZHANG, L., PENNEFATHER, P., AND CARLEN, P. Reversible inhibition of I_K, I_{AHP}, I_h and I_{Ca} currents by internally applied gluconate in rat hippocampal pyramidal neurones. *Pflügers Arch.* 433: 343–350, 1997.

WICHMANN, T., BERGMAN, H., AND DELONG, M. R. The primate subthalamic nucleus. III. Changes in motor behavior and neuronal activity in the internal pallidum induced by subthalamic inactivation in the MPTP model of parkinsonism. *J. Neurophysiol.* 72: 521–530, 1994.